ACS APPLIED MATERIALS & INTERFACES

Freie Universität Berlin

Subscriber access provided by UB + Fachbibliothek Chemie | (FU-Bibliothekssystem)

Article

A hybrid energy harvester consisting of piezoelectric fibers with largely enhanced 20V for wearable and muscle-driven applications

Yiin-Kuen Fuh, Jia-Cheng Ye, Po Chou Chen, Hsi-Chun Ho, and Zih-Ming Huang

ACS Appl. Mater. Interfaces, **Just Accepted Manuscript** • DOI: 10.1021/acsami.5b03955 • Publication Date (Web): 03 Jul 2015

Downloaded from http://pubs.acs.org on July 7, 2015

Just Accepted

"Just Accepted" manuscripts have been peer-reviewed and accepted for publication. They are posted online prior to technical editing, formatting for publication and author proofing. The American Chemical Society provides "Just Accepted" as a free service to the research community to expedite the dissemination of scientific material as soon as possible after acceptance. "Just Accepted" manuscripts appear in full in PDF format accompanied by an HTML abstract. "Just Accepted" manuscripts have been fully peer reviewed, but should not be considered the official version of record. They are accessible to all readers and citable by the Digital Object Identifier (DOI®). "Just Accepted" is an optional service offered to authors. Therefore, the "Just Accepted" Web site may not include all articles that will be published in the journal. After a manuscript is technically edited and formatted, it will be removed from the "Just Accepted" Web site and published as an ASAP article. Note that technical editing may introduce minor changes to the manuscript text and/or graphics which could affect content, and all legal disclaimers and ethical guidelines that apply to the journal pertain. ACS cannot be held responsible for errors or consequences arising from the use of information contained in these "Just Accepted" manuscripts.

ACS Publications
High quality. High impact.

ACS Applied Materials & Interfaces is published by the American Chemical Society.
1155 Sixteenth Street N.W., Washington, DC 20036
Published by American Chemical Society. Copyright © American Chemical Society.
However, no copyright claim is made to original U.S. Government works, or works produced by employees of any Commonwealth realm Crown government in the course of their duties.

A hybrid energy harvester consisting of piezoelectric fibers with largely enhanced 20V for wearable and muscle-driven applications

Yiin-Kuen Fuh[1*], Jia-Cheng Ye[2], Po-Chou Chen[1], Hsi-Chun Ho[1], Zih-Ming Huang[1]

[1]*Department of Mechanical Engineering, National Central University, No.300, Jhongda Rd., Jhongli District, Taoyuan City 32001, Taiwan (R.O.C.)*

[2]*Energy Engineering, National Central University, No.300, Jhongda Rd., Jhongli District, Taoyuan City 32001, Taiwan (R.O.C.)*

Corresponding author: Dr. Yiin-Kuen Fuh

Mailing Address: Department of Mechanical Engineering, National Central University, No.300, Jhongda Rd., Jhongli District, Taoyuan City 32001, Taiwan (R.O.C.)

Telephones: +886- 03-4267305 (office)

Fax: +886- 03-4254501

E-mail: michaelfuh@gmail.com

Abstract

We present a polyvinylidene fluoride (PVDF) nanogenerator (NG) with advantages of direct-writing and in-situ poling via near-field electrospinning (NFES), which is completely location addressable and substrate independent. The maximum output voltage reached 20 V from the three layers piled NGs with serial connections, and the maximum output current can exceed 390 nA with the parallel integration setup. Linear superposition and switching-polarity of current and voltage tests were validated by the authentic piezoelectric output. Nanofibers (NFs)-based devices with a length ~5 cm can be easily attached on the human finger under folding-releasing at ~ 45 ° and the output voltage and current can reach 0.8 V and 30 nA, respectively. This work based on NFs can potentially have a huge impact on harvesting various external sources from mechanical energies.

Keywords: near-field electrospinning, nanogenerator, energy harvester, nanofibers, polyvinylidene fluoride, muscle-driven

Introduction

Renewable and non-exhaustible resources energy such as wave power and wind have rekindled considerable intensive interest to prevent the global warming and resources dwindling. However, solar and thermal energies are highly dependent on time, location and not universally ubiquitous and accessible. Therefore, human-motion-based energy harvesting has attracted tremendous interest due to growing popularity of portable smart electronics as an independently self-sufficient and sustainable power source. Progress in nanogenerators (NG) for portable electronics[1] and self-powered nanosystems has become more technologically feasible due to the advancement of extremely low power consumption nanoelectronics. Furthermore, harvesting energy from negligible human action or tiny body movement is very promising since it is location independent, especially for personal electronics, human based activities and associated mechanical movement is the comparatively reliable and environmentally independent. The first significant contribution could trace back to 2006, the piezoelectric zinc oxide (ZnO) nanowires (NWs) arrays were demonstrated to convert tiny mechanical energy into electrical energy. To deflect aligned NWs by using a conductive atomic force microscope tip in contact mode and ~8mV ~0.5 pW were generated from a single NW actuation.[2] Furthermore, a scalable sweeping-printing method was proposed to fabricate stretchable and high output NG; an open-circuit voltage up to 2.03 V, close-circuit current of 100nA and a peak output power density of ~ 11 mW/cm^3 was achieved.[3] Poly(vinylidene fluoride) (PVDF) is another alternative material for piezoelectricity and nanofibers (NFs) with diameters ranging from 70 to 400 nm produced by electrospinning. Domain switching and

associated ferro-/piezo-electric properties of the electrospun PVDF fibers have shown well-defined ferroelectric and piezoelectric properties.[4] Considering the hybrid device consisting of a piezoelectric PVDF NFs NG and a flexible enzymatic biofuel cell, the open loop voltage of 15 to 20 mV and the short circuit current of 0.2 to 0.3 nA were obtained.[5] Recently, near-field electrospinning (NFES) is proven to be able to achieve the direct-write capability such that well controllable ability and precise patterning to deposit substantial NFs in a continuous, direct-write, and controllable process.[6] Geometric patterns such as grid arrays and circular shapes on wide and flat areas can be reliably obtained[7] with well controllable manner. In recent years, rapid progress has been developed on the fundamental mechanism of NFs deposition via NFES such as controlled formation of multiple jets[8] and associated self-organization behavior based on the wave propagation theory.[9] For bio-compatible material such as chitosan/poly(ethylene oxide), successfully direct-write and well-aligned NFs deposited in a continuous fashion was demonstrated.[10] For functional material such as piezoelectric PVDF, a comparative study utilizing both continuous near-field electrospinning (CNFES) and conventional electrospinning processes of electrospun PVDF-based membranes (EPMs) was also investigated in terms of fiber dimension, processing parameters, crystallinity, Differential scanning calorimetry (DSC), Fourier transform infrared spectroscopy (FTIR) etc.[11] On the recent application of NFES, fabrication of monolithic polymer nanofluidic channels via NFES electrospun NFs as sacrificial templates was demonstrated and 550-800nm nanofluidic channels can be reliably fabricated based on this template method.[12] Another interesting area is for cell morphology and spreading control and direct-write, highly aligned chitosan-poly(ethylene oxide) NF patterns is successfully demonstrated.[13] In addition, based on the NW and percolation theory, the ultra-long metallic microwires was pursued to replace the brittle indium tin oxide (ITO) and pattern transfer technique has been developed based on the process of an electrospun NF template, sputtered metallic layers and soft stamp transfer of aligned metal nano/microwires as flexible transparent electrodes.[14] Applying the NFES technique as a viable tool to fabricate the NGs was initially pioneered and a direct-write PVDF NG with high energy conversion efficiency was successfully demonstrated. Possibly owing to fewer defects of the NFES process and a higher degree of crystallinity, the electrical outputs of 0.5 - 3 nA and 5 - 30 mV for a single NF for the efficiency as high as 21.8% was achieved, as compared with the film counterpart of 0.5-4%.[15] In order to amplify the harvested energy, PVDF electrospun NFs arranged in a series and/or in parallel with patterned comb-shape gold electrodes were also presented and a peak current of 35nA and peak voltage of 0.2mV were measured.[16] Significant progress toward a usable output in the range of ~V was newly made. The continuous deposition of PVDF NFs poses a strict challenge and a restricted operating region was recognized, resulting in the

massively parallel aligned nano/microfibers-based harvester fabricated via oriented and in situ poled NFES. The major advancement to aligned and oriented poled 500 microfibers deposited continuously in parallel and serial configurations are able to produce a peak output current of ~300nA and a voltage of ~1.7 V, which the magnitude increment is two to three orders in both current/voltage outputs when compared NFES setup of a single NF to the similar amount of nano/microfibers with post poling treatment.[17] For the integrated hybrid cell with various energy sources such as thermoelectric and solar cells, previously demonstrated mechanical harvesters are mainly focused on triboelectric nanogenerators (TENG), while the applications are self-powered sensors, water splitting without an external power source[18] and energy storage in a Li-ion battery for lighting up LEDs[19]

Experimental

In this paper, we demonstrate an in-situ poled and direct-write NG via NFES process to massively fabricate PVDF NFs arrays and fully encapsulated on a flexible substrate. Highly reproducible and integrated multiple NGs connected in serial and parallel are experimentally capable of increasing output voltage and current. In serial connections, the three-layer stacked NGs can reach maximum output voltage of 20 V. Alternatively, the maximum output current 390 nA can be achieved from the parallel integration of the same device. The size of the fabricated NG was 3.5 cm × 1 cm × 2 μm. The electrical outputs (VL) is measured to be 4V. While the power output reaches the optimized output power of 5.34 μW at matched resistance of 1.5 MΩ. The power density amount 7629 μW/cm3 has been achieved. As a comparison, the generated power density is on the similar magnitude of previously published fiber-based generator and compared favorably with MEMS-based counterpart.[9]

Finally, the muscle-driven capabilities of developed NG devices are also demonstrated for a fiber-based wearable technology and opens up the potentially promising solution of harvesting the energy from human activity with minimal intervention. Moreover, a hybrid cell is demonstrated, which is capable of harvesting energy from tiny mechanical motions.

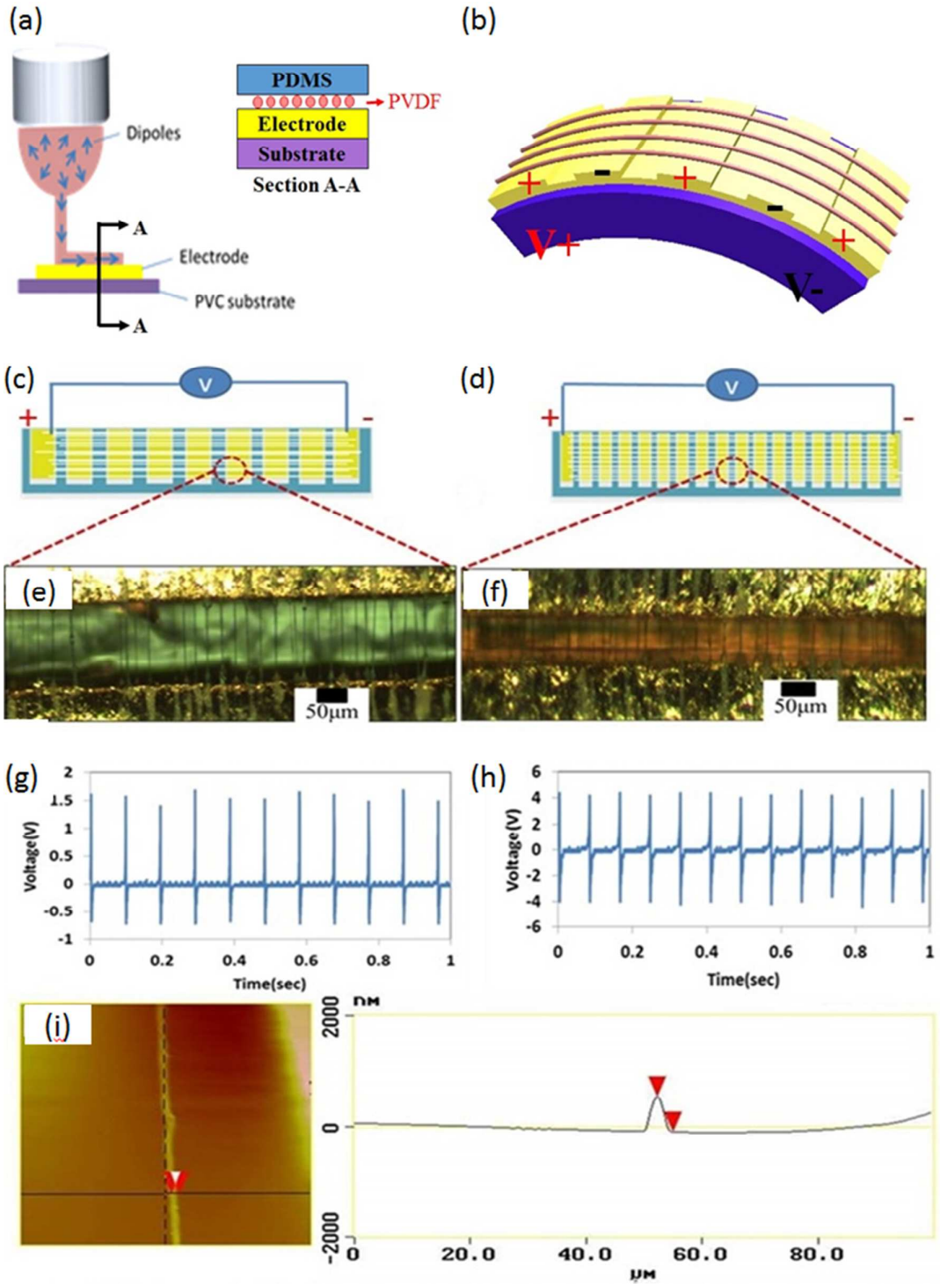
(a)
Dipoles
PDMS
PVDF
Electrode
Substrate
Section A-A
A
Electrode
PVC substrate
A
(b)
V+
V-
(c)
V
+
-
(d)
V
+
-
(e)
50μm
(f)
50μm
(g)
Voltage(V)
Time(sec)
(h)
Voltage(V)
Time(sec)
(i)
nm
2000
0
-2000
0
20.0
40.0
60.0
80.0
μm

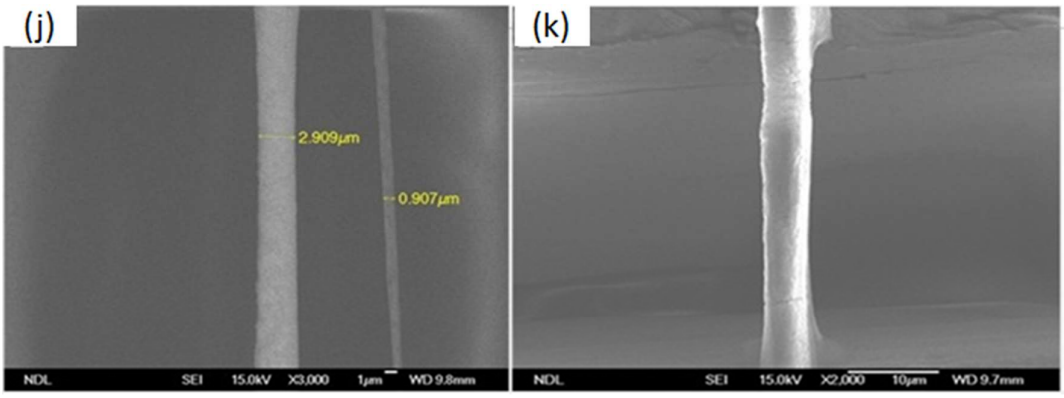

Fig.1 (a) Schematic of the in-situ, direct-write and electrical poling PVDF fibers via NFES. The mechanical stretching forced fibers deposited onto a flexible PVC substrate to construct the NG. (b) Mode of deformation schematic. When loaded mechanical deformation on the substrate, a corresponding piezoelectric potential in the NFs can be elicited by the tensile strain, where the "±" signs indicate the polarity of the piezoelectric potential. Fig.1 (c-d) Schematic diagram of the NG design. Different electrode gap on the same flexible substrate, respectively (e)A total of about 500 parallel NFs and 10 electrode pairs have been fabricated on top of a flexible substrate. (f) A total of about 500 parallel NFs and 40 electrode pairs have been fabricated on top of a flexible substrate. (g-h) According to the different electrode pairs, the output voltage of NG voltage superposition in serial configuration. (i) Atomic Force Microscope (AFM) images of PVDF nanofibers via direct-write NFES technique. (j) Scanning electron microscope (SEM) images of electrospun PVDF nanofibers of two different diameters fabricated via direct-write NFES manner. There are diameter variation of NFs as shown at 0.9 and 2.9μm, respectively. (k) Another zoomed SEM photomicrograph showing NFs with a diameter of ~4.8μm.

Fig.1 (a) shows the schematic diagram of the direct-write and NFES PVDF fibers with in-situ electrical poling and mechanical stretching steps. In the serial/parallel configuration electrical voltage and current superposition can be accomplished effortlessly via the adjustment of the electrode gap distance. Mode of the deformation and the current/voltage scaling-up superposition principle for the electrospun NFs are integrated as one massive-arrays energy gathering apparatus. As applied mechanical deformation onto the substrate, a corresponding piezoelectric potential in the NFs can be induced, where the "±" signs represent the polarity of the local piezoelectric potential created inside the NFs in situ. Fig.1 (c-d) illustrates the schematic diagram of the electrode gap effect in serial (current) and parallel (voltage) configuration, respectively, suspending multiple fibers across two or more copper contact electrodes (made of 55 μm-thick copper foil) on an insulation polyvinyl chloride (PVC) substrate

deposited by the direct-write NFES process. [15] The typical electrode separation distance is in the range of 50–120 μm and the direct-write technique is comprehending by using an x–y stage (Parker, Inc.) to control the deposition rate and course of the substrate during the NFES process, resulting in a desirable pattern at specific regions of interest. PVDF solution is prepared by using N,N-Dimethylformamide (DMF) (Sigma-Aldrich) as solvent for PVDF powder (Sigma-Aldrich, Mw = 534000), acetone and fluorosufactant (ZONYL® UR) are added to optimize the evaporation rate and surface tension of the solution, respectively 10. The electrospinning process parameters used in this case are 16 wt% PVDF, solvent (DMF:acetone with 1:1 weight ratio), 4 wt% fluorosufactant (Capstone® FS-66), 1.2 mm for the needle-to-collector distance, 1.44 kV for the electrospinning voltage. The size of the fabricated NG was 3.5 cm × 1 cm × 2 μm. Encapsulation with PDMS was applied to secure structural stability.

Fig.1 (e-f) A total of about 500 parallel NFs were electrospun on top of the 10 and 40 metallic electrodes, respectively with different working gaps, 120μm and 50μm, respectively which were between two electrodes. When dynamic strain/stress was applied by deforming the flexible substrate, there were about 5000 active working contacts for 10 metallic electrodes and 20000 active working contacts for 40 metallic electrodes to harvest charges generated from these PVDF NFs. The as-spun PVDF NFs have average diameters ranging from 900nm to 2.5μm. Fig.1 (g-h) investigates the performance of output voltage that can be greatly enhanced by superpositioning a number of electrode pairs in a series configurations. The experimental results were obtained by measuring approximately 5000 rows and 20000 rows of NFs arrays, respectively. Then a cyclic stretching-releasing deformation at a strain of 0.5% and 10 Hz by a linear motor was used to periodically deform the electrospun NG. For example, the NG output voltage was connected in a series, leading to an output voltage of 1.5 and 4 V when the substrate was stretched and released repeatedly. The corresponding AFM images were shown in Fig.1 (i) indicating the diameter was c.a. 2.5μm, which is the average diameter of electrospun NFs. Previously, an experimental validation on the spinnability of NFES PVDF NFs was investigated and facilitated here such that the stable NFES spinning window of continuous and large-area deposition was reproducibly carried out.[17] However, the continuous deposition of PVDF NFs was identified as a limiting and pretty narrow operating region, at the sacrifice of diameter variation of NFs. We intentionally choose the most obviously different diameters of NFs and perform the characterization. The corresponding SEM images were shown in Fig.1 (j) of two PVDF NFs fabricated sequentially via direct-write NFES processing conditions, indicating the diameter was c.a. 2.9 μm and 0.9μm, respectively. Fig.1 (k) shows another fiber with diameter c.a. 4.8μm, which is one of the largest diameters and the uniformity of electrospun fibers can be further

improved by tightly controlling the processing conditions such as precise electric field via constant tip-to-electrode distance and solution conductivity, viscosity as well as surface tension.

For the crystallinity characterization of PVDF NFES electrospun nanofibers and related polarized phase, the spectroscopic evidence for the effective transformation from paraelectric to a high fraction of induced ferroelectric phase had been recently identified and proven.[20]

The key factors contribute to the highly efficient α→β phase due to the oriented unit cells of hydrogen and fluoride (CH_2–CF_2) polar structure, β-phase is primarily responsible for PVDF's piezoelectric response. In order to largely enhanced the β-phase PVDF, electrical poling and mechanical stretching processes are indispensable to directionally align the dipoles in the crystalline PVDF structures. Transformation has been found to be the indispensable steps of mechanical stretching and electric poling processes during the NFES process as shown in Supplementary information Fig. S1. Previously posed challenge on continuous deposition of PVDF nanofibers was overcome and a pretty narrow operating region was identified [17] as shown in Supplementary information Fig. S-2. The spectroscopic evidence such as XRD and FTIR to demonstrate phase information of the produced NFs are shown in Supplementary Information of Figs.S3-S4 respectively. From the above data, the NFES direct-write electrospun PVDF fibers have these common phases (Nonpolar α-phase and the polar β- and γ-phases) that were observed. Among these phases, the polar β-phase is the most important evidence of piezoelectric property.[20] We also tested the Performance stability, besides process improvement. In Supplementary Information Fig. S5 the stability of NG can be consistently observed.

Results and Discussion

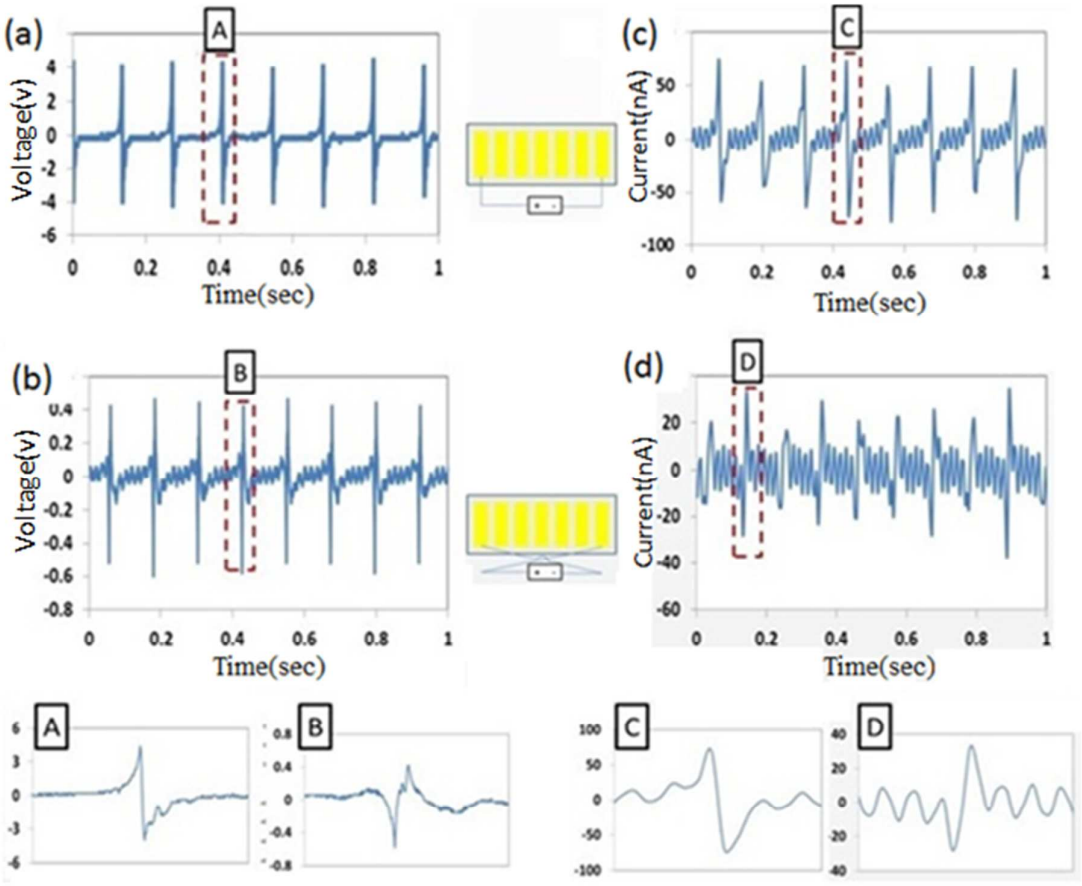

Fig.2 A polarity test under forward and reverse connections for (a, b) voltage output from NG (c, d) Current power output from NG. The magnified pattern of one single bending and release process is illustrated in the bottom plots A-D. Peak voltage was measured to be about 4V in the forward connection and 0.4V in the reverse connection, the peak current was measured to be 75nA in the forward connection and 30nA in the reverse connection, respectively.

For the forward/reverse connection of voltage measurements, the positive/negative and negative/positive probes of the measurement system are connected to the positive/positive and negative/negative electrodes of the NG, respectively. The detail experimental setup regarding the results presented in Fig. 2-4 can be found in Fig.S6. Considering the individual electrospun fiber, the piezoelectric coefficients has been characterized and an average piezoelectric coefficient d_{33} of −63.25 pm/V, which is comparable to the previous reported values of NFES fibers [25] and is significantly larger than the PVDF thin-films [26-29]. The detail of piezoelectric characterization can be found in Supplementary Information Fig.S7. In addition, we also did some simulation to obtain the piezoelectric coefficients of single poled PVDF fiber and the

results of the deformation of the PVDF fiber can be found in Supplementary Information Fig.S11 and S12.

Fig.2 (a) shows the results for voltage output of one NG. The insets illustrate the corresponding connection configurations. As the NG is bent inward cyclically to induce the stretching states, corresponding positive peaks can be measured consistently. Similarly, when the substrate is released and the NG returns to a free state, a negative electric peak is concurrently measured. The mechanism with strain-induced piezoelectric potential and related electric signal generation can be found elsewhere.[15,17] The switching-polarity test is generally recognized to identify if the signal is an artifact or not, such that the true electricity output from the piezoelectric property of the NG can be proven. Experimentally, opposite polarity of voltage meter and NG are connected, i.e., the positive and negative probes of the voltage meter are connected to the negative and positive ends of the NG, respectively as shown in Fig.2 (b). The reversal output signal is experimentally measured as the stretching of the NG produces a negative pulse and vice versa. Additionally, the magnitude difference between the signal of forward connection and reverse connection is also observed in our NFs-based NG, as similar phenomena was reported previously on zinc oxide (ZnO) NWs based NGs.[21] The electric current output of the NGs is presented in Fig.2(c)(d). In the same phase, in-synchronization of voltage and current output is observed such that a positive/negative current signal is generated when the NG is stretched/released. Fig. 2 (d) shows the output current and switching polarity is also experimentally fulfilled. The inset at the bottom of Fig.2 A-B illustrates the peak voltage and measured to be ~4V, ~0.4V in the forward and reverse connections, respectively. Similar to the voltage measurement, the current measurement result is plotted in Fig.2C-D. The polarity check for the piezoelectric response was confirmed since the shape of the response was flipped. The peak currents in the forward and reverse connections were ~75 nA and ~30 nA, respectively.

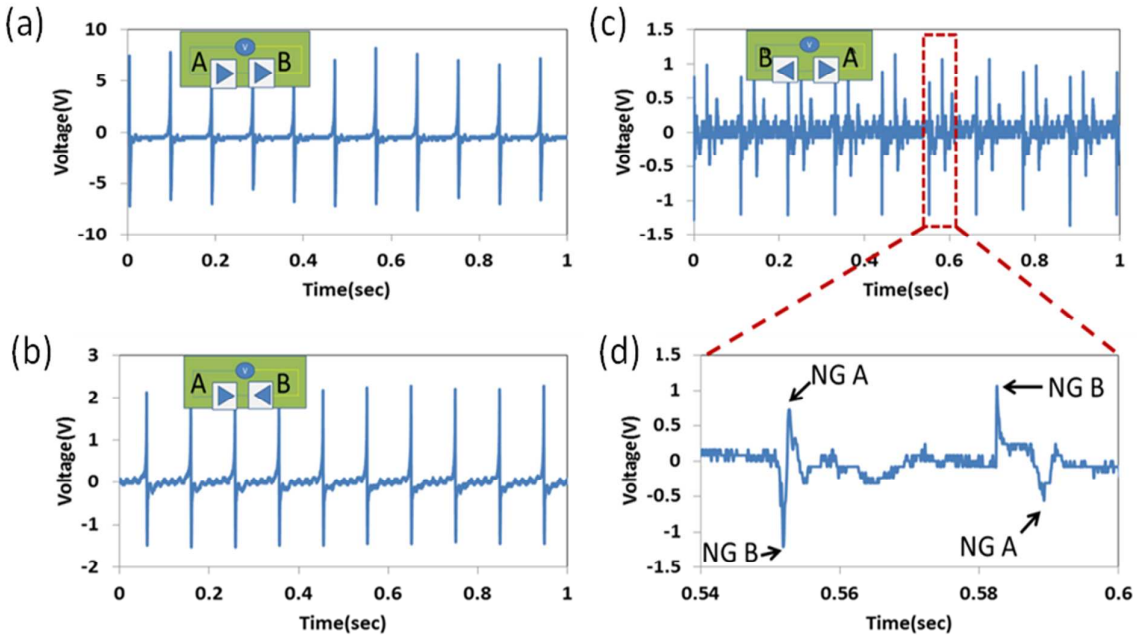

Fig.3 (a-b) Superposition of the voltage scale-up or cancelation effect is demonstrated in serial connection of NG A and NG B. The connection configurations of the NGs of all insets are in reference to the measurement system. (c) Intentionally deformed, the two NGs reversely connected in serial in a mode of slightly off synchronization and resulted in voltage output. The inset illustrates the connection configuration of the NGs. (d) an enlarged view of two outputs and double peaks in (c) to illustrate the abrupt switch in output voltage for NG A & B respectively.

The capability of voltage scale-up can be demonstrated as the two NGs are serially connected as shown in Fig.3 (a) and Fig.3 (b). The superposition principle of voltage is satisfied when two NGs are connected in the same direction, as the final output can noticeably increase and basically follows the fundamental electric circuit theory. In comparison, the voltage output can be significantly reduced when two NGs are connected in opposite directions. In addition, the serially connected NGs must also meet the requirement of switching-polarity test. On the other hand, the demonstration of full electrical signal superposition can only rely on the precise synchronization between two NGs such that the induced strain of either the deformed or released state should operate simultaneously. Any small off-synchronization or a little delay in the deformation will result in the distinctly different outputs of the two NGs. We experimentally demonstrate the phenomena of a pair of positive-negative peaks by oppositely connected two serial NGs as shown in Fig.3 (c). When two NGs are stretched or released in a fashion that one immediately follows the other, two NGs

sequentially generated the double peaks signals that are opposite in sign and slightly off- synchronized. In this case, NG B is bending first and follows the bending of NG A before the completion of NG B bending. This purposely off- synchronized implementation will result in the first double peak with a negative sign due to reversal connection. In what follows, the NG B releasing completion and the release of NG A, another peak with a positive sign is observed, in a fashion similar to the first double peak and reversal connection. Any measurement artifact and incompatibility of linear superposition rule can be further validated as the two positive-negative peaks as presented in Fig. 3(d). We also using the well-accepted method to characterize the true signals for output voltage and current of integrated NGs, a linear superposition of either voltage/current can be satisfied for the two NGs in serial/parallel connection, respectively (Supplementary Information of Figs.S8-S9). Furthermore, the switching-polarity tests are also conformed for the two NGs, fully in agreement with published data and indicate the true signals are obtained from the fabricated NGs.

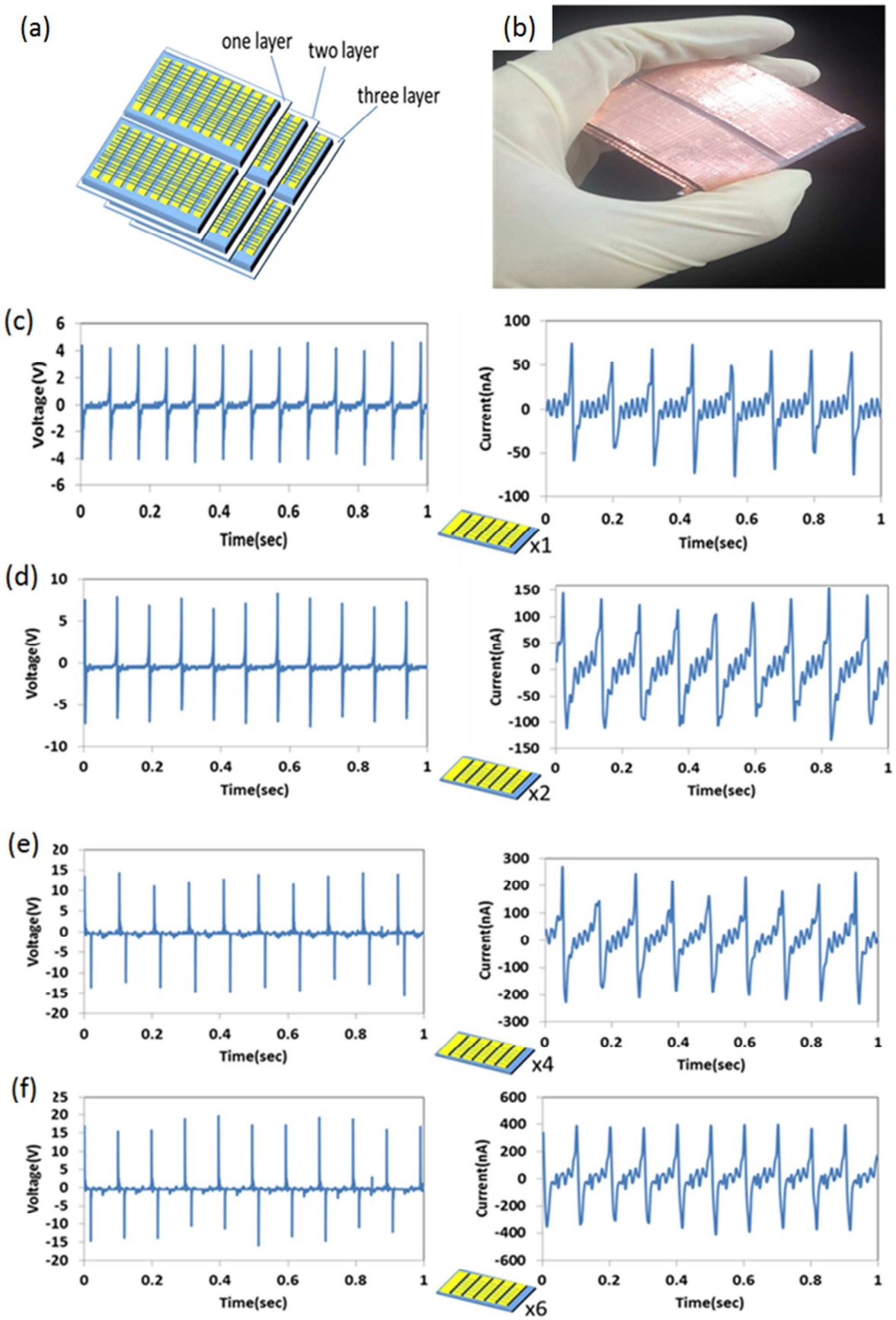
(a)
one layer
two layer
three layer
(b)
(c)
Voltage(V)
Time(sec)
Current(nA)
Time(sec)
x1
(d)
Voltage(V)
Time(sec)
Current(nA)
Time(sec)
x2
(e)
Voltage(V)
Time(sec)
Current(nA)
Time(sec)
x4
(f)
Voltage(V)
Time(sec)
Current(nA)
Time(sec)
x6

Fig.4 A largely enhanced electrical output NG device integrated in parallel for voltage and in serial for current. (a) Demonstration of the integrated NG to the feasibility of scale-up for promoting the output voltage and current. The number of integrated layers in the parallel and serial configurations is experimentally demonstrated to have a direct impact on the output voltage and current. (b) Photographic image of the NG device integrated in parallel and serial with three layers, i.e. six units of NGs. Output voltage and current of NGs integrated in serial and in parallel configuration, respectively with (c) one unit (d) one layer, (e) two layers, and (f) three layers. Please note that one layer in (d)-(f) contains two units of NGs

For enhancing and scaling-up of both output voltage and current, the proposed direct-write, in-situ poled NFES NGs can be effortlessly integrated in series and in parallel on a PVC substrate. To demonstrate the feasibility of scale-up in output voltage, NGs integrated serially with three layers on the PVC substrate, as shown in Fig.4 (a), is used to characterize the electrical performance. We gradually increase the number of serially integrated layers and perform measurement sequentially to guarantee successful integration in serial. [22] The fabricated NFs-device is encapsulated in PDMS polymer on a PVC substrate as shown in Fig.4 (b) of the optical image. We fabricate 6 units of NFs-based generators and one of the electrical outputs is measured to be 4V and 75 nA, respectively for voltage and current as shown in Fig.4 (c). We also combine two units on the same structural layer to improve the output due to the simultaneously induced external force on the integrated layers in series. As such, the increment of output voltage was found due to the increasing number of layers via summing up the external piezoelectric potential. The voltage superposition can be distinctly demonstrated by serial integration as the output voltage increases with the number of serially integrated layers under the same conditions. As the number of integrated layers increases from 1 to 3, corresponding to a total of 6 units of NGs, their output voltages are effectively enhanced from 7.5, 15 and to 20V, respectively. On the other hand, the output current enhancement can be achieved for the device integrated in parallel. For the layer of parallel integration, the measured output current is ~145nA as shown in Fig.4 (d). Concurrently integrated two- or three layered NGs led to an increased output current of 260 nA and 390 nA, respectively, as shown in Fig. 4 (e-f). The superposition demonstrated is not exactly the sum of the individual output in the measured series and parallel integrated NGs and the reason may be attributed to variation in diameters of deposited NFs and successful deposition rate of individually fabricated NG. Nonetheless, the direct-write, in-situ poled and large-area deposition as well as facile scale-up possibility of the series and parallel integration can be convincingly increased along with output voltage and current.

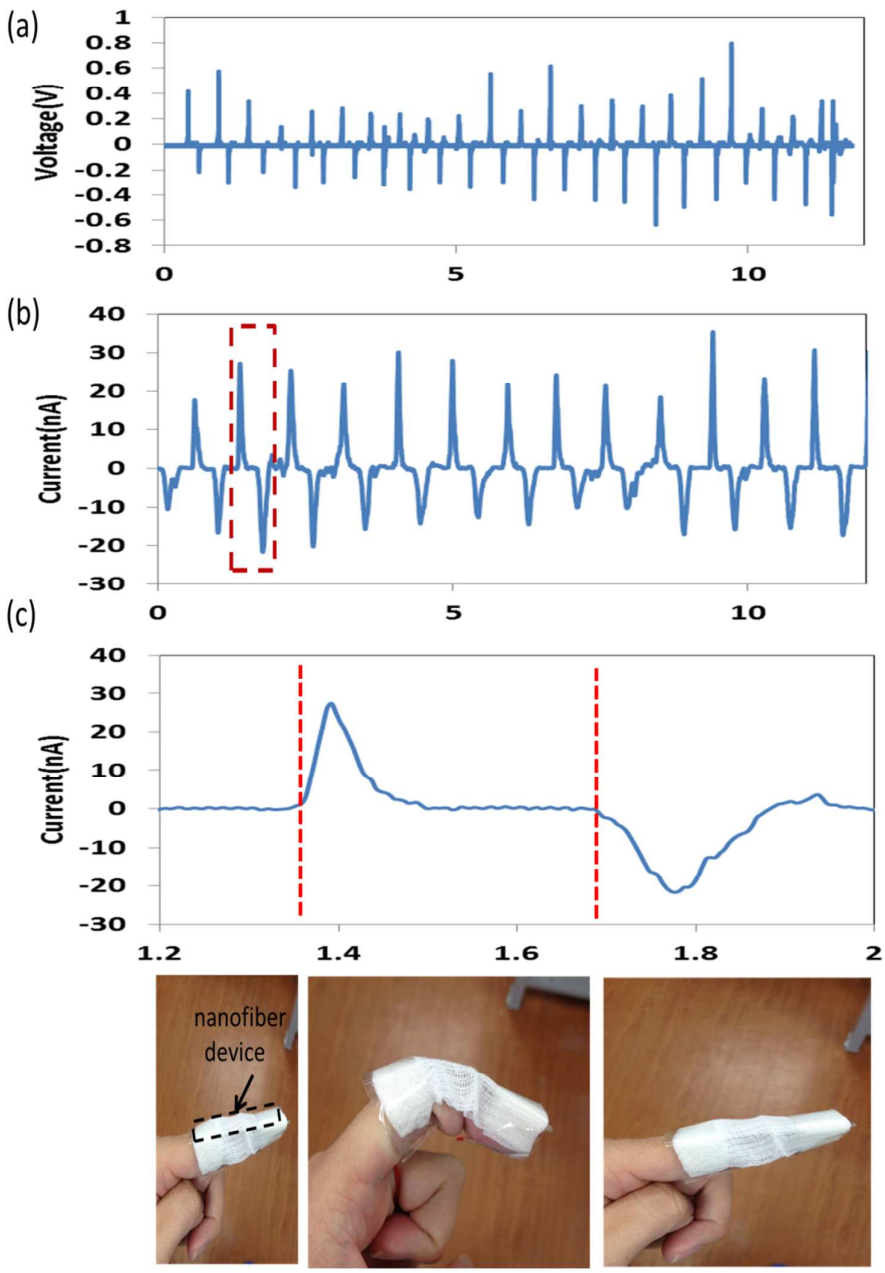

Fig.5 Human finger-enabled NG using direct-write, in-situ poled NFs and corresponding electrical measurements. The NFs device is direct-write on the thin copper film with a predefined electrode pattern and fixed on textile substrate of woven cotton with dimension of 7.4cm × 3.9cm × 0.8mm and mass density of 175 g/m^2, encapsulated with PDMS and attached on the finger. Experimentally, a uniform stress is induced as the finger folds and released during the measurements. (a) Multiple events of finger folding-releasing actions and corresponding voltage outputs of a NFs device. (b) Current output of a NFs device generated by bending and stretching out the finger. (c) A current output occurred on the event of the bending and stretching out action of the finger. The finger was held at an angle of ~ 45 °.

Wearable electronics self-powered from human activity such as walking and muscle movement are very promising as previously demonstrated.[23-24] Furthermore, a structurally 3-D spacer and functionally piezoelectric all-fiber textiles has also been developed as a wearable NG.[30] Here we demonstrate our NFs-based NG can be easily deposited on the flexible textiles at a specific location with predefined electrodes and attached onto a human finger for scavenging the human movement. The encapsulated PDMS protecting layer is employed to prevent any undesired electrical noise from device contacts to the human skin directly. Our NFs-based device exhibited the voltage and current outputs of ~ 0.8V and 30nA, respectively, truthfully in–synchronized with the human finger motion, as shown in Fig.5 (a-b). The bottom plots in Fig.5 (c) show a firmly attached NFs-based device on a finger and concurrently experiencing strain from the bending and stretching out actions of the finger. The novel structure of our NFs-based device can be further improved by integrating another NFs-template transparent electrode[14] to achieve, in the field of wearable electronics, a completely flexible energy harvester that unnoticeably scavenges tiny mechanical activity of living creatures with very little obstruction.

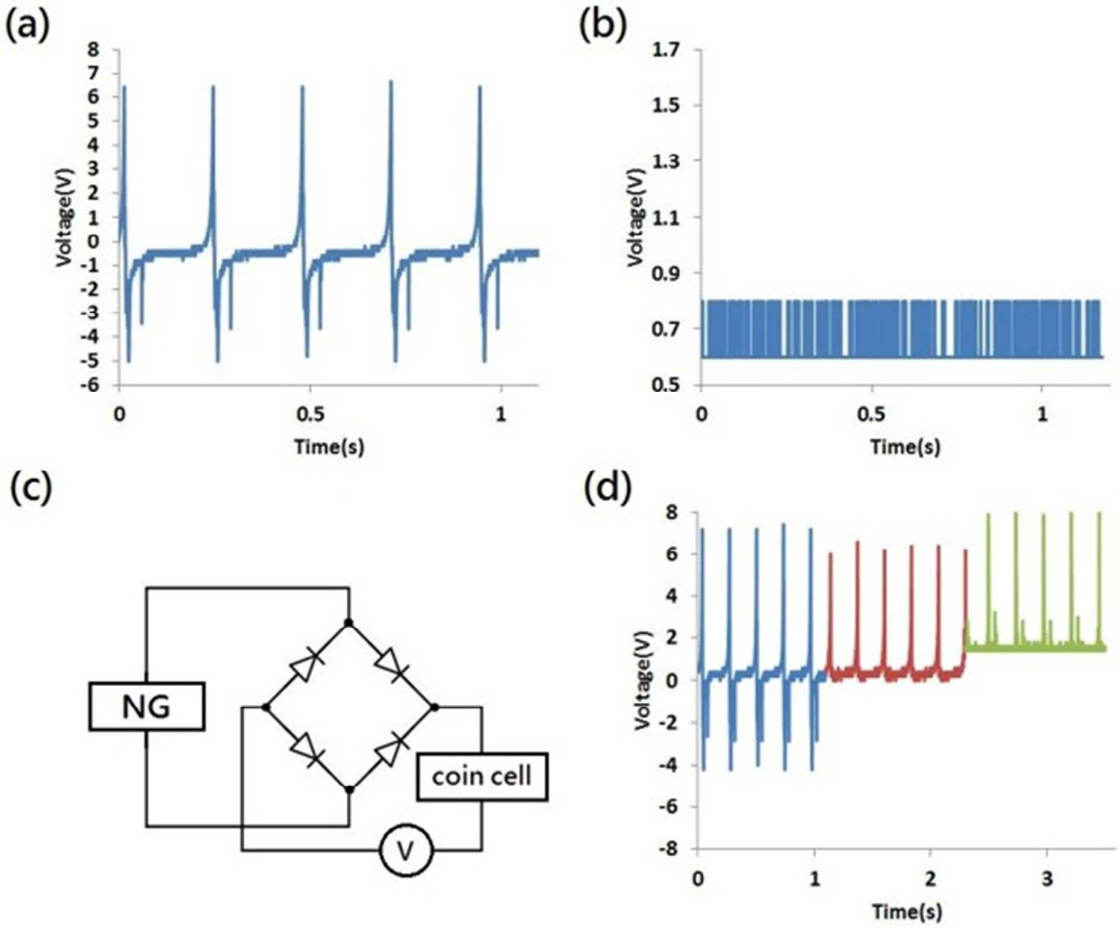

Fig. 6 (a) Output voltage of NG with one layer NFs array in serial configuration. (b) Output voltage of coin cell (c) Schematic diagram of the connection between the NG and the coin cell. (d) Output voltage of the hybrid coin cell and NG.

Fig. 6(a) and (b) show the output performance of the fabricated NG and coin cell (Maxell,LR44,1.5V/60mAh), respectively. The corresponding output voltage is about 6.5 V and 0.7V, respectively. Fig. 6(c) shows a schematic diagram of the hybrid energy cell with a bridge rectification circuit. Both the NG and the coin cell were connected for converting the alternating current to the direct current. Fig. 6(c) shows the hybrid energy cell schematic of both the NG and the coin cell, where a full bridge rectification circuit was connected with the NG for alternating current to direct current conversion. Fig. 6(d) shows the output voltages of the NG before (blue) and after (red) rectification as well as the hybrid energy cell (green) respectively in three different colors. It can be well demonstrated that the output voltage signals of the hybrid cell are rectified to be positive and much larger than the single energy harvester due to the superposition effect. In addition, we also scavenged the voltage and current of NGs with two layers NFs array in serial configuration for the full rectification in Supplementary Information Fig. S10. Fig. S10 show the same result (positive voltage

and current signals after rectified), but higher output power than NG with only one layer configuration.

Conclusion

Structurally robust, reproducibly scalable, substrate-independent and large-area NGs utilizing the NFES direct-write technique to massively align piezoelectric PVDF NFs on flexible substrates have been successfully fabricated. The particular properties of in-situ electrical poling and mechanical stretching can promise the scaling-up of the piezoelectric potentials with minimal effort to integrate NGs in parallel and/or series for improvement of output voltage and current. The NGs that comprised 20000 rows of well-aligned PVDF NFs are able to create a peak output voltage of ~4 V and a current reaching 75nA. Furthermore, a highly promising and feasible power source for wearable electronics is demonstrated as the three-layers integrated NGs can reach the maximum output voltage and current up to 20V and 390 nA, respectively. Two main contributions are summarized. First, the proposed device is two to three orders of magnitude increment in both voltage and current outputs when compared with either a single NF or similar NFES setup with post poling treatment due to opposite poling direction for a similar amount of NFs.[15] Second, by attaching our NFs-based device (with a length of approximately ~5 cm) on the human finger under folding-releasing at ~ 45 °, the output voltage and current can reach 0.8 V and 30 nA, respectively. In addition, we have also demonstrated an NFs-based hybrid energy cell that can harvest mechanical. Therefore, this NFs-based device and integrated hybrid cell can provide a highly promising renewable energy source for future wearable electronics that harvests the mechanical motion of humans with very minimal intervention.

Supporting Information

SEM, XRD and FTIR of the fabricated device with parallel aligned NFs were performed and compared between the original PVDF powder, NFES PVDF fiber, and conventional electrospinning PVDF thin film. Deformation simulation of center displacement as a function of electric field were employed and compared with experimental measurements of various fiber diameters of single PVDF fiber such that the piezoelectric constant of deposited NFs can be deduced. This information is available free of charge via the Internet at http://pubs.acs.org/.

References

1. Wang, Z. L.; Zhu, G.; Yang, Y.; Wang, S.; Pan, C., Progress in Nanogenerators for Portable Electronics , *Mater. Today*, **2012**, 15, 532-543.

2. Wang, Z. L.; Song, J. H., Piezoelectric Nanogenerators Based on Zinc Oxide Nanowire Arrays, *Science*, **2006**, 312, 242-246.

3. Zhu, G.; Yang, R.; Wang, S.; Wang, Z. L., Flexible High-Output Nanogenerator Based on Lateral ZnO Nanowire Array, *Nano Lett.*, **2010**, 10, 3151-3155.

4. Baji, A.; Mai, Y. W.; Li, Q.; Liu, Y., Electrospinning Induced Ferroelectricity in Poly(Vinylidene Fluoride) Fibers , *Nanoscale*, **2011**, 3, 3068-3071.

5. Hansen, B. J.; Liu, Y.; Yang, R.; Wang, Z. L., Hybrid Nanogenerator for Concurrently Harvesting Biomechanical and Biochemical Energy , *ACS Nano*, **2010**, 4, 3647-3652.

6. Sun, D.; Chang, C.; Li, S.; Lin, L., Near-Field Electrospinning, *Nano Lett.*, **2006**, 6, 839-842.

7. Chang, C.; Limkrailassiri, K.; Lin, L., Continuous Near-Field Electrospinning for Large Area Deposition of Orderly Nanofiber Patterns, *Appl. Phys. Lett.*, **2008**, 93, 123111.

8. Fuh, Y. K.; Hsu, H. S., Controlled Formation of Multiple Jets and Nanofibers Deposition Via Near-Field Electrospinning Process, *Int. J. Nonlinear Sci. Numer. Simul.*, **2010**, 11, 979-984.

9. Fuh, Y. K.; Lien, L. C., Self-Organization of Multiple Jets in Near-Field Electrospinning Process, *Micro. Nano. Lett.*, **2012**, 7, 1088-1091.

10. Fuh, Y. K.; Chen, S.; Jang, S. C., Direct-Write Well-Aligned Chitosan-Poly(Ethylene Oxide) Nanofibers Deposited Via Near-Field Electrospinning, *J. Macromol. Sci., Part A: Pure Appl.Chem.*, **2012**, 49, 845-850.

11. Fuh, Y. K.; Lien, L. C.; Jang, S. C., A Comparative Study of PVDF Nanofibrous Membranes Prepared by Continuous Near-Field and Conventional Electrospinning Processes, *Micro. Nano. Lett.*, **2012**, 7, 376-379.

12. Fuh, Y. K.; Hsu, H. S., Fabrication of Monolithic Polymer Nanofluidic Channels Via Near-Field Electrospun Nanofibers as Sacrificial Templates, *J. Micro/Nanolithogr., MEMS, MOEMS.*, **2011**, 10, 043004.

13. Fuh, Y. K.; Chen, S.; He, Z., Direct-Write Highly-Aligned Chitosan-Poly(Ethylene Oxide) Nanofiber Patterns for Cell Morphology and Spreading Control, *Nanoscale Res. Lett.*, **2013**, 8, 97.

14. Fuh, Y. K.; Lien, L. C., Pattern Transfer of Aligned Metal Nano/Micro Wires as Flexible Transparent Electrodes Using An Electrospun Nanofibers Template, *Nanotechnology*, **2013**, 24, 055301.

15. Chang, C.; Tran, V. H.; Wang, J.; Fuh, Y. K.; Lin, L., Direct-Write Piezoelectric Polymeric Nanogenerator With High Energy Conversion Efficiency , *Nano Lett.*, **2010**, 10, 726-731.

16. Chang, J.; Lin, L., Large Array Electrospun PVDF Nanogenerators on A Flexible Substrate, *Transducers*, **2011**, 747-750.

17. Fuh, Y. K.; Chen, S. Y.; Ye, J. C., Massively Parallel Aligned Microfibers-Based Harvester Deposited Via in Situ, Oriented Poled Near-Field Electrospinning, *Appl. Phys. Lett.*, **2013**, 103, 033114.

18. Yang, Y.; Zhang, H.; Lin, Z-H; Liu, Y.; Chen, J.; Lin, Z.; Zhou, Y. S.; Wonga, C. P.; Wang, Z. L., A Hybrid Energy Cell for Self-Powered Water Splitting, *Energy Environ. Sci.*, **2013**, 6, 2429-2434.

19. Yang, Y.; Zhang, H.; Chen, J.; Lee, S.; Hou, T-C.; Wang, Z. L., Simultaneously Harvesting Mechanical and Chemical Energies by A Hybrid Cell for Self-Powered Biosensors and Personal Electronics, *Energy Environ. Sci.*, **2013**, 6, 1744-1749.

20. Lei, T.; Cai, X.; Wang, X.; Yu, L.; Hu, X.; Zheng, G.; Lv,W.; Wang, L.; Wu, D.; Sun, D.; Lin, L., Spectroscopic Evidence for A High Fraction of Ferroelectric

Phase Induced in Electrospun Polyvinylidene Fluoride Fibers, *RSC Adv.*, **2013**, 3, 24952-24958.

21. Yang, R.; Qin, Y.; Lin, C.; Dai, L.; Wang, Z. L., Characteristics of Output Voltage and Current of Integrated Nanogenerators, *Appl. Phys. Lett.*, **2009**, 94, 022905.
22. Lee, S.; Hong, J.; Xu, C.; Lee, M.; Kim, D.; Lin, L.; Hwang, W.; Wang,Z. L., Toward Robust Nanogenerators Using Aluminum Substrate, *Adv. Mater.*, **2012**, 24, 4398-4402.
23. Lee, M.; Chen, C-Y.; Wang, S.; Cha, S. N.; Park, Y. J.; Kim, J. M.; Chou, L-J.; Wang, Z. L., A Hybrid Piezoelectric Structure for Wearable Nanogenerators, *Adv. Mater.*, **2012**, 24, 1759-1764.
24. Lee, S.; Bae, S-H.; Lin, L.; Yang, Y.; Park, C.; Kim, S-W.; Cha, S. N.; Kim, H.; Park, Y. J.; Wang, Z. L., Super-Flexible Nanogenerator for Energy Harvesting from Gentle Wind and as An Active Deformation Sensor, *Adv. Funct. Mater.*, **2012**, 23, 2445-2449.
25. Pu, J.; Yan, X. J.; Jiang, Y. D.; Chang, C.; Lin, L. W., Piezoelectric Actuation of Direct-Write Electrospun Fibers, *Sens. Actuators, A*, **2010**, 164, 131-136.
26. Dargaville, T. R.; Celina, M.; Chaplya, P. M., Evaluation of Piezoelectric PVDF Polymers for Use in Space Environments. Part I: Temperature Limitations, *J. Polym. Sci., Part B: Polym. Phys.*, **2005**, 43, 1310–1320.

27. Ye, Y.; Jiang, Y.; Wu, Z.; Zeng, H., Phase Transitions of Poly(Vinylidene Fluoride) Under Electric Fields, *Integr. Ferroelectr.*, **2006**, 80, 245–251.

28. He, X.; Yao, K., Crystallization Mechanism and Piezoelectric Properties of Solution-Derived Ferroelectric Poly(Vinylidene Fluoride) Thin Films, *Appl. Phys. Lett.*, **2006**, 89, 112909.

29. Guthner, P.; Ritter, T.; Dransfeld, K., Temperature Dependence of The Piezoelectric Constant of Thin PVDF and P(VDF-TrFE) Films, *Ferroelectrics*, **1992**, 127, 7–11.

30. Soin, N.; Shah, T. H.; Anand, S. C.; Geng, J.; Pornwannachai, W.; Mandal, P.; Reid, D.; Sharma, S.; Hadimani, R. L.; Bayramol, D. V.; Siores, E., Novel "3-D Spacer" All Fibre Piezoelectric Textiles for Energy Harvesting Applications, *Energy Environ. Sci.*, **2014**, 7, 1670-1679.

Table Of Contents (TOC) graphic